Eur. Phys. J. B **14**, 509–513 (2000)

THE EUROPEAN PHYSICAL JOURNAL B

EDP Sciences

Charge-carrier density collapse in $La_{0.67}Ca_{0.33}MnO_3$ and $La_{0.67}Sr_{0.33}MnO_3$ epitaxial thin films

W. Westerburg[1], F. Martin[1], P.J.M. van Bentum[2], J.A.A.J. Perenboom[2], and G. Jakob[1,a]

[1] Institut für Physik, Johannes Gutenberg-Universität Mainz, 55099 Mainz, Germany
[2] Research Institute for Materials and High Field Magnet Laboratory, University of Nijmegen, 6252 ED Nijmegen, The Netherlands

Received 22 July 1999 and Received in final form 7 October 1999

Abstract. We measured the temperature dependence of the linear high field Hall resistivity ρ_H of $La_{0.67}Ca_{0.33}MnO_3$ ($T_C = 232\,K$) and $La_{0.67}Sr_{0.33}MnO_3$ ($T_C = 345\,K$) thin films in the temperature range from 4 K up to 360 K in magnetic fields up to 20 T. At low temperatures we find a charge-carrier density of 1.3 and 1.4 holes per unit cell for the Ca- and Sr-doped compound, respectively. In this temperature range electron-magnon scattering contributes to the longitudinal resistivity. At the ferromagnetic transition temperature T_C a dramatic drop in the number of charge-carriers n down to 0.6 holes per unit cell, accompanied by an increase in unit cell volume, is observed. Corrections of the Hall data due to a non saturated magnetic state will lead a more pronounced charge-carrier density collapse.

PACS. 71.38.+i Polarons and electron-phonon interactions – 73.50.Jt Galvanomagnetic and other magnetotransport effects (including thermomagnetic effects) – 75.30.Vn Colossal magnetoresistance

1 Introduction

The colossal magnetoresistance (CMR) in ferromagnetic perovskite manganites has reattracted strong theoretical and experimental interest. These materials show metallic-like transport at low temperatures in the ferromagnetically ordered phase. In the paramagnetic regime above the metal-insulator transition temperature a polaronic conduction takes place and an electronlike, thermally activated Hall coefficient was found [1,2]. This is in agreement with the expectations from polaron hopping. Lowering of the temperature will lead to the formation of a polaron band and a 'metallic' transport, *i.e.* positive temperature coefficient of the resistivity. In the vicinity of the metal-insulator transition the polaronic bands are stabilised by external magnetic fields. Therefore we investigated the linear high-field Hall resistivity in magnetic fields up to 20 T. The experimentally determined increase of the Hall coefficient at the metal-insulator transition translates into a charge-carrier density collapse (CCDC) in the band picture. While such a CCDC in low magnetic field was proposed by Alexandrov and Bratkovsky [3] due to formation of immobile bipolarons, our high field results indicate the influence of the structural phase transition at the Curie temperature on the band structure.

[a] e-mail: jakob@mail.uni-mainz.de

2 Experimental

Thin films of $La_{0.67}Sr_{0.33}MnO_3$ (LSMO) were prepared by pulsed laser deposition (KrF Laser, $\lambda = 248\,nm$). As substrates we used (100) $SrTiO_3$ and (100) LSAT ($(LaAlO_3)_{0.3}$-$(Sr_2AlTaO_6)_{0.7}$ untwinned). The optimised deposition conditions were a substrate temperature of 950 °C in an oxygen partial pressure of 14 Pa and annealing after deposition at 900 °C for 1 h in an oxygen partial pressure of 600 hPa. $La_{0.67}Ca_{0.33}MnO_3$ (LCMO) was deposited by magnetron sputtering on (100) MgO substrates. Further details on preparation and characterisation are published elsewhere [4]. In X-ray diffraction in Bragg-Brentano geometry only film reflections corresponding to a (l00) orientation of the cubic perovskite cell are visible for both compounds. The LSAT substrates ($a_0 = 3.87\,Å$) have a small lattice mismatch to the Sr-doped films (3.89 Å). Rocking angle analysis shows epitaxial a-axis oriented growth with an angular spread smaller than 0.03°. The in-plane orientation was studied by ϕ-scans of (310) reflections. The cubic perovskite axes of the films are parallel to that of the substrates with an angular spread smaller than 1°. The temperature dependence of the unit cell volume of the LCMO sample was determined measuring in- and out of plane lattice constants using a helium flow cryostat with Beryllium windows on a four circle X-ray diffractometer.

The samples were patterned photolithographically to a Hall bar structure. For measuring in the temperature regime from 4 K up to room temperature we used

Table 1. Curie temperatures, charge-carrier densities, residual resistivities and fitting parameters of equation (1) for $La_{0.67}Ca_{0.33}MnO_3$ and $La_{0.67}Sr_{0.33}MnO_3$ thin films.

Compound	T_C (K)	n(4 K) (holes/unit cell)	ρ_0 (mΩcm)	ρ_2/ρ_0 (10^{-6} K^{-2})	$\rho_{4.5}$(0 T)/ρ_0 (10^{-11} K$^{-4.5}$)	$\rho_{4.5}$(8 T)/ρ_0 (10^{-11} K$^{-4.5}$)
LCMO	232	1.3	0.294	68	256	134
LSMO	345	1.4	0.139	54	41	36

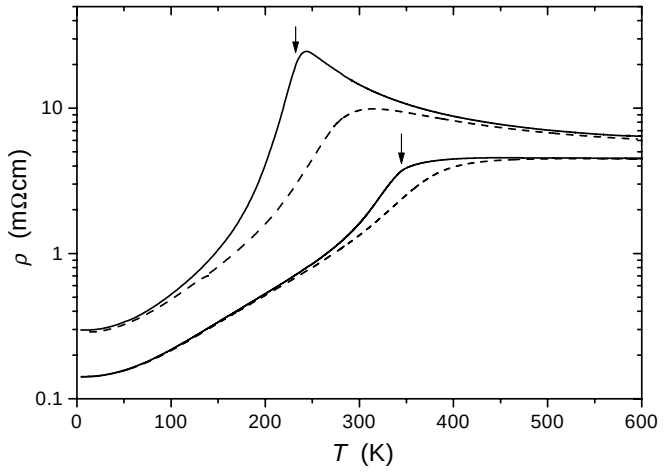

Fig. 1. Resistivities in zero field (solid lines) and in 8 T magnetic field (dashed lines) as functions of temperature. The arrows at 232 K (345 K) indicate the Curie temperatures for $La_{0.67}Ca_{0.33}MnO_3$ ($La_{0.67}Sr_{0.33}MnO_3$).

a standard 12 T magnet cryostat. An 8 T superconducting coil and a 20 T Bitter type magnet system, both with room temperature access, have been used for measurements above 270 K. The procedure used for measuring the Hall effect is described in detail elsewhere [5]. The magnetic moments of the films were measured with a SQUID magnetometer in a small field of $\mu_0 H = 20$ mT.

3 Results and discussion

In Figure 1, the longitudinal resistivities of the Ca- and Sr-doped compounds $\rho_{xx}(T)$ are shown in zero field (solid lines) and in 8 T (dashed lines). The Curie temperatures of both samples are indicated by arrows, 232 K for LCMO and 345 K for LSMO, respectively. For LCMO the maximum in resistivity is close to T_C. For very high and very low temperatures the curves are asymptotic, *i.e.* the magnetoresistance vanishes. The resistivity as function of temperature is up to $T/T_C = 0.6$ given by

$$\rho = \rho_0 + \rho_2 T^2 + \rho_{4.5} T^{4.5}. \quad (1)$$

The parameters of equation (1), obtained by fitting the experimental data, are listed in Table 1. The quadratic contribution is not changed in presence of a high magnetic field. This was also observed by Snyder *et al.* [1] while Mandal *et al.* [6] found both factors to be magnetic field dependent. One possible origin of a quadratic temperature dependence of the resistivity is due to emission and absorption of magnons. But in this case a magnetic field dependence would be expected. Furthermore in these processes an electron reverses its spin and changes its momentum. However, in the manganites spin flip processes play no role at low temperatures due to strong spin splitting of the states. Therefore we attribute this T^2 dependent term to electron-electron scattering in a Fermi liquid. The term proportional to $T^{4.5}$ results from electron-magnon scattering in the double exchange theory of Kubo and Ohata [7]. In these scattering events the electron spin is conserved, while momentum is exchanged between the electron and magnon system. Its contribution to the resistivity in equation (1) is proportional to

$$\rho_{4.5} = \frac{\epsilon_0 \hbar}{e^2 k_F} \frac{1}{S^2} (a k_F)^6 \left(\frac{m}{M}\right)^{4.5} \left(\frac{k_B}{E_F}\right)^{4.5} \quad (2)$$

with the manganese spin S and the lattice constant a. A small correction relevant only for effective mass ratio $M/m > 1000$ is neglected in equation (2). The strong temperature dependence of this scattering mechanism is partly determined by the number density of excited magnons $\propto T^{3/2}$. In magnetic field this term is suppressed reflecting the increased magnetic order. Evaluating $\rho_{4.5}$ in the free electron approximation yields a value 3 orders of magnitudes smaller than experimentally determined. However, due to the strong influences of effective mass renormalizations in equation (2) effective mass ratios of M/m in the range 3–6 will give quantitative agreement.

For the Ca-doped compound the transport above T_C is thermally activated [2] and can be described by small polaron hopping [8]. The Sr-doped compound has a lower resistivity and a lower magnetoresistance (MR), because the absolute MR decreases with increasing T_C [9]. Here, the resistivity above T_C is described by a crossover between two types of polaron conduction [1]. Scattering of polarons by phonons just above T_C results in a positive $d\rho/dT$, so that in the case of LSMO T_C does not coincide with the maximum in resistivity. The Curie temperature is at a lower value (see Fig. 1) where an anomaly in the temperature dependence of the resistivity is seen [10].

The transverse resistivity ρ_{xy} in a ferromagnet as a function of a magnetic field B is expressed by

$$\rho_{xy} = R_H B + R_A \mu_0 M, \quad (3)$$

with the magnetisation M, ordinary Hall coefficient R_H, and anomalous Hall coefficient R_A [11]. In our thin film geometry the demagnetisation factor N is close to unity and therefore the magnetic induction $B = \mu_0[H + (1 - N)M]$ is given by $B = \mu_0 H$. The Hall resistivity $\rho_{xy}(\mu_0 H)$ for

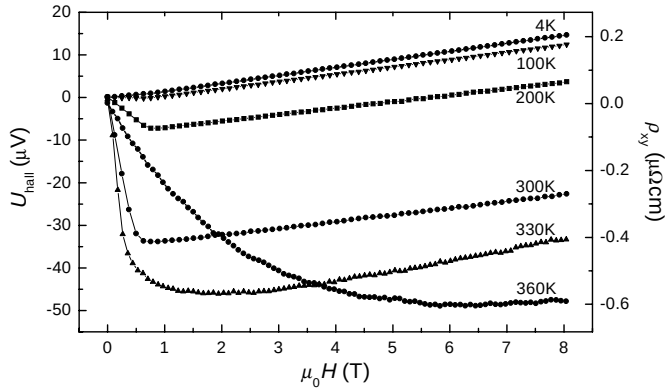

Fig. 2. The Hall resistivity ρ_{xy} and the Hall voltage $U_{\rm H}$ as a function of applied magnetic field at various temperatures for $La_{0.67}Sr_{0.33}MnO_3$.

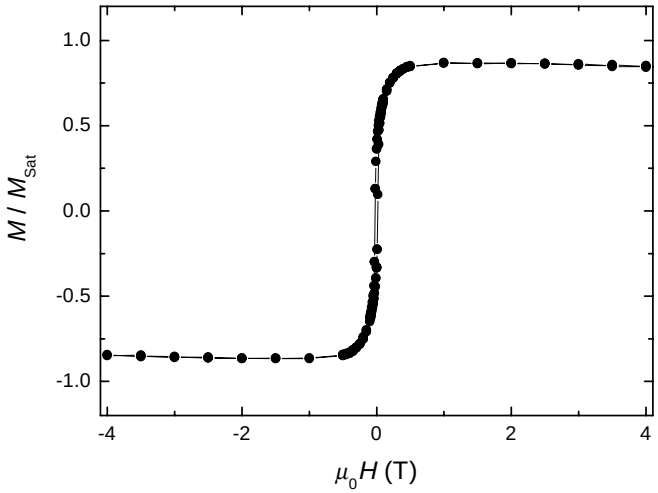

Fig. 3. Ferromagnetic hysteresis curve for the LCMO film measured at 20 K normalised to the expected saturation value. The error of the measured magnetic moments is smaller than the symbol size. However, the uncertainty in film thickness leads to a possible error of 10% in the scale factor. The diamagnetism of the substrate is responsible for the small decrease of the magnetic moment at high magnetic fields.

LSMO for several constant temperatures as a function of magnetic field H is shown in Figure 2. At low magnetic fields a steep decrease of the Hall voltage $U_{\rm H}$ is seen, which is strongest at $T_{\rm C}$ and becomes less pronounced at low temperatures and above $T_{\rm C}$. This part is dominated by the increase in magnetisation with magnetic field. Therefore the electronlike anomalous Hall effect, $R_{\rm A} > R_{\rm H}$, dominates the Hall voltage:

$$\frac{{\rm d}\rho_{xy}}{{\rm d}(\mu_0 H)} = \frac{t}{I}\frac{{\rm d}U_{\rm H}}{{\rm d}(\mu_0 H)} = R_{\rm H} + R_{\rm A}\frac{{\rm d}M}{{\rm d}H}, \qquad (4)$$

with the film thickness t and current I. At higher fields the magnetisation saturates and the linear positive slope is due to the ordinary Hall effect. This behaviour is very similar to the Ca-doped compound, if one compares the reduced temperatures $T/T_{\rm C}$ [5]. The initial slopes ${\rm d}\rho_{xy}/{\rm d}(\mu_0 H)(H \to 0)$ are highest at the Curie-temperature for both compounds in agreement with the Berry phase theory of the anomalous Hall effect [12]. The temperature dependence of the electronlike anomalous Hall constant is thermally activated, similar to the longitudinal resistivity and consistent with the theory of Friedman and Holstein [13]. This was also observed by Jaime *et al.* [14] and provides another strong evidence of small polarons in manganites. More details to the interpretation of the anomalous Hall effect are published elsewhere [2,5].

In the following, we consider the high-field regime where the slopes ${\rm d}\rho_{xy}/{\rm d}(\mu_0 H)$ are positive and constant indicating hole conduction. The saturation of the magnetic moment at high magnetic fields was confirmed by SQUID measurements of the samples at low temperatures. In Figure 3 we show the hysteresis loop of the LCMO sample. Clearly small fields are sufficient to achieve nearly full saturation magnetisation. From an alignment of all the Mn spins one expects $M_{\rm Sat} = 3.67$ Bohr magnetons per unit cell. Due to the different demagnetisation factors in magnetisation and transport measurements the saturation field in the Hall measurements will be enhanced by $\mu_0 M_{\rm Sat} \approx 0.7$ T to approximately $\mu_0 H_{\rm Sat} = 1.2$ T, well below the field range where the data are evaluated. Even if a residual increase of the film magnetisation will take place at high fields, it will have a negligible contribution to the slope ${\rm d}\rho_{xy}/{\rm d}(\mu_0 H)$ at low temperatures, where the anomalous Hall coefficient vanishes. For 4 K, we obtain in a single-band model 1.4 holes per unit cell for LSMO. A smaller value ≈ 1 hole per unit cell was found by Asamitsu and Tokura on single crystals [15] while for a thin film a value of 2.1 was reported [1]. For Ca-doped thin films similar values were found [5,16] and in an $La_{2/3}(Ca,Pb)_{1/3}MnO_3$ single crystal the hole density was determined to 2.4 holes per unit cell [17]. This large charge-carrier density in manganites requires the concept of a partly compensated Fermi surface [18].

To investigate the charge-carrier concentration just above $T_{\rm C}$, it is important to have as high magnetic field as possible in order to saturate the magnetisation. Therefore, we performed for LCMO Hall effect measurements up to 20 T. In this field a positive linear slope ${\rm d}\rho_{xy}/{\rm d}\mu_0 H$ can be observed up to $T/T_{\rm C} = 1.3$. The Hall resistivites $\rho_{xy}(\mu_0 H)$ are shown in Figure 4. For clarity several curves ($T = 275$ K, 300 K, 305 K, 310 K and 315 K) are omitted. Just above $T_{\rm C}$ at 285 K it is possible to almost saturate the magnetisation of the sample and a broad field range with a linear positive slope remains to evaluate $R_{\rm H}$. The fit of the slope is seen in Figure 4 by the dashed line. At 350 K ($T/T_{\rm C} = 1.5$) the shift of the minimum in the Hall voltage to higher fields allows no longer a quantitative analysis of $R_{\rm H}$.

Assuming full saturation of the magnetisation in high magnetic field the charge-carrier concentration $n = 1/eR_{\rm H}$ as a function of the reduced temperature $T/T_{\rm C}$ for LCMO (circles) and LSMO (triangles) is plotted in Figure 5. LCMO has a constant carrier concentration at low temperatures, whereas for LSMO n increases with

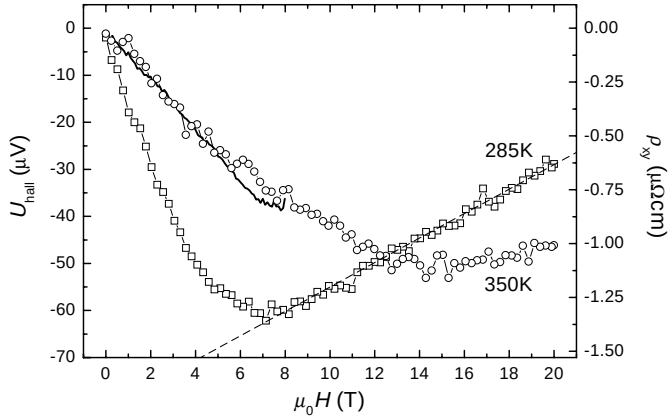

Fig. 4. Measured Hall resistivity ρ_{xy} and Hall voltage U_{H} as function of magnetic field at temperatures of 285 K (squares) and 350 K (circles) for $La_{0.67}Ca_{0.33}MnO_3$ in a 20 T Bitter magnet. Five measured curves were omitted for clarity. The lines are measurements in an 8 T superconducting magnet and show the correspondence between different experimental setups. The dotted line is a fit of the linear slope.

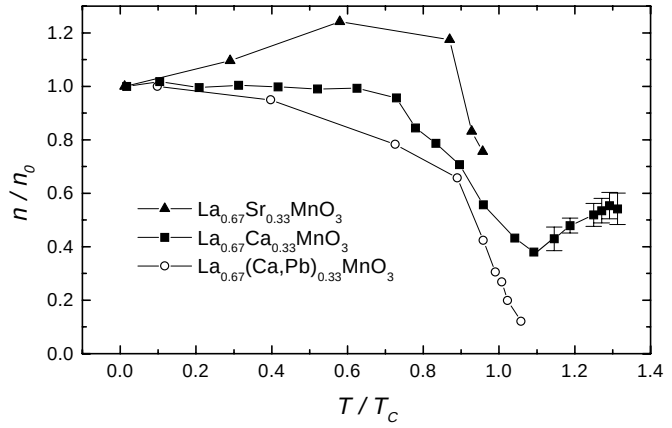

Fig. 5. Apparent normalised charge-carrier density $n \propto (\mathrm{d}\rho_{xy}/\mathrm{d}(\mu_0 H))^{-1}$ of $La_{0.67}Ca_{0.33}MnO_3$ (filled squares, $T_{\mathrm{C}} = 232$ K) and $La_{0.67}Sr_{0.33}MnO_3$ (filled triangles, $T_{\mathrm{C}} = 345$ K) as a function of the reduced temperature T/T_{C}. For the measurements in the 12 T superconducting magnet errors are comparable to symbol size. In the 20 T Bitter magnet electrical noise leads to enhanced error bars for the linear slopes $(\mathrm{d}\rho_{xy}/\mathrm{d}(\mu_0 H))^{-1}$ as indicated. Additionally we show data from reference [17] (open circles, $T_{\mathrm{C}} = 287.5$ K) on a single crystal of $La_{0.67}(CaPb)_{0.33}MnO_3$.

temperature. But for both doped manganites clearly a decrease of n at the Curie temperature is seen. This temperature dependence of n seems to be a characteristic behaviour of the manganites in the vicinity of T_{C}, since this was also observed by Wagner *et al.* [19] in thin films of $Nd_{0.5}Sr_{0.5}MnO_3$, indirectly by Ziese *et al.* [20] in thin films of $La_{0.67}Ca_{0.33}MnO_3$ and $La_{0.67}Ba_{0.33}MnO_3$ and by Chun *et al.* [17] in single crystals of $La_{0.67}(CaPb)_{0.33}MnO_3$. The latter data are also shown as open symbols in this figure for comparison. According to Figure 5 above T_{C} the number of charge carriers seems to reincrease. The error bars

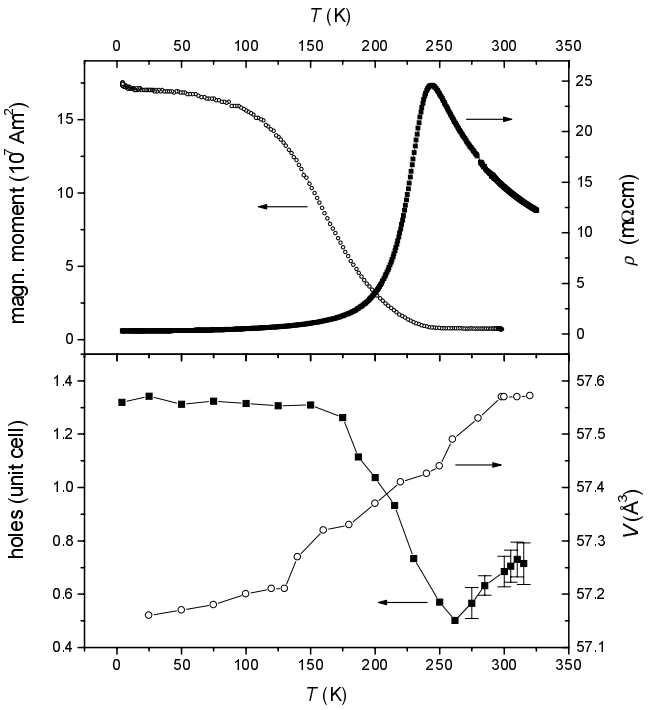

Fig. 6. Temperature dependence of magnetisation, resistivity, charge-carrier density and unit cell volume for a thin film of $La_{0.67}Ca_{0.33}MnO_3$.

indicate the accuracy of the determination of the linear slopes $\mathrm{d}\rho_{xy}/\mathrm{d}(\mu_0 H)$, as shown for $T = 285$ K in Figure 4. However, well above the Curie temperature the magnetisation of the sample cannot be saturated in experimentally accessible magnetic fields. From equation (4) it is obvious, that a linearly increasing magnetisation in this paramagnetic regime will not affect the linearity of the slope $\mathrm{d}\rho_{xy}/\mathrm{d}(\mu_0 H)$ but change its value. Without quantitative knowledge of the anomalous Hall coefficient R_{A} and the sample magnetisation $M(T, H)$ it is not possible to separate this contribution. Nevertheless, since the sign of the anomalous Hall contribution is electronlike, it is clear that the apparent charge-carrier density shown in Figure 5 has to be corrected to *lower* values above the Curie temperature, thus *enhancing* the CCDC.

This CCDC indicates strong changes in the electronic distribution function close to the Fermi energy. Since coincidence of structural, magnetic and electronic phase transitions has been reported for $La_{1-x}Ca_xMnO_3$ with $x = 0.25$ and 0.5 [21], we investigated the temperature dependence of lattice constants, magnetisation, longitudinal resistivity, and transversal resistivity for the same sample. Figure 6 shows a compilation of the results. The charge-carrier density is constant up to $0.7\,T_{\mathrm{C}}$. In this temperature range the resistivity follows equation (1) and the volume of the unit cell increases slowly with temperature. The fact that the CCDC is accompanied by a strong increase in unit cell volume and longitudinal resistivity and a decay of the spontaneous magnetisation shows

the coincidence of structural, magnetic, and electronic phase transitions in $La_{0.67}Ca_{0.33}MnO_3$.

As the transport in the manganites above T_C is dominated by polaron hopping [2,14] we want to discuss the relation between our experimental observation of the CCDC and the polaronic CCDC as proposed recently by Alexandrov and Bratkovsky [3]. They worked out the theory for a CCDC due to a phase transition of mobile polarons to immobile bipolaronic pairs. At low temperatures the charge-carriers form a polaronic band. With increasing temperature the polaronic bandwidth decreases due to the increase in electron phonon coupling. Depending on the polaron binding energy and the doping level a first or second order phase transition to a bound bipolaronic state takes place. At still higher temperatures thermal activation of the bipolarons leads to a reincrease of the number of mobile polarons. Indeed their calculated temperature dependence of the number density of mobile polarons in zero field is very similar to our data shown in Figure 5. However, in this model the density of mobile polarons around T_C is a strong function of magnetic field, which is responsible for the colossal magnetoresistivity. In high fields the polaronic CCDC is strongly reduced, since the formation of bound bipolarons is suppressed and accordingly the number of mobile polarons remains almost constant at T_C. Therefore our observation of a CCDC in high fields cannot be identified with the CCDC due to bipolaron formation, but is related to structural changes. We cannot determine the charge-carrier density in the low field regime due to strong anomalous Hall contributions. In their presence the type of phase transition proposed by Alexandrov and Bratkovsky cannot be verified by Hall effect measurements.

4 Summary

We performed detailed Hall effect measurements in high magnetic fields in LCMO and LSMO thin films. The charge-carrier concentration was investigated as a function of temperature below and above the Curie temperature. In the low temperature range, where the charge-carrier density is constant, we identified electron-magnon scattering in the longitudinal resistivity. At the ferromagnetic transition temperature a charge-carrier density collapse was observed for both compounds. The data indicate a simultaneous structural, magnetic and electronic phase transition in doped manganite thin films.

This work was supported by the Deutsche Forschungsgemeinschaft through project JA821/1-3 and the European Union TMR-Access to Large Scale Facilities Plan.

References

1. G.J. Snyder, R. Hiskes, S. DiCarolis, M.R. Beasley, T.H. Geballe, Phys. Rev. B **53**, 14434 (1996); Appl. Phys. Lett. **69**, 4254 (1996).
2. G. Jakob, W. Westerburg, F. Martin, H. Adrian, Phys. Rev. B **58**, 14966 (1998).
3. A.S. Alexandrov, A.M. Bratkovsky, Phys. Rev. Lett. **82**, 141 (1999).
4. G. Jakob, F. Martin, W. Westerburg, H. Adrian, J. Magn. Magn. Mater. **177-181**, 1247 (1998).
5. G. Jakob, F. Martin, W. Westerburg, H. Adrian, Phys. Rev. B **57**, 10252 (1998).
6. P. Mandal, K. Bärner, L. Haupt, A. Poddar, R. von Helmolt, A.G.M. Jansen, P. Wyder, Phys. Rev. B **57**, 10256 (1998).
7. K. Kubo, N. Ohata, J. Phys. Soc. Jpn **33**, 21 (1972).
8. D. Emin, T. Holstein, Ann. Phys. (NY) **53**, 439 (1969).
9. K. Khazeni, Y.X. Jia, L. Lu, V.H. Crespi, M.L. Cohen, A. Zettl, Phys. Rev. Lett. **76**, 295 (1996).
10. Y. Tokura, A. Urushibara, Y. Moritomo, T. Arima, A. Asamitsu, G. Kido, N. Furukawa, J. Phys. Soc. Jpn **63**, 3931 (1994).
11. R. Karplus, J.M. Luttinger, Phys. Rev. **95**, 1154 (1954).
12. J. Ye, Y.B. Kim, A.J. Millis, B.I. Shraiman, P. Majumdar, Z. Tešanović, `cond-mat/9905007` preprint (1999).
13. L. Friedman, T. Holstein, Ann. Phys. (N.Y.) **21**, 494 (1963).
14. M. Jaime, H.T. Hardner, M.B. Salamon, M. Rubenstein, P. Dorsey, D. Emin, Phys. Rev. Lett. **78**, 951 (1997), J. Appl. Phys. **81**, 4958 (1997).
15. A. Asamitsu, Y. Tokura, Phys. Rev. B **58**, 47 (1998).
16. P. Matl, N.P. Ong, Y.F. Yan, Y.Q. Li, D. Studebaker, T. Baum, G. Doubinina, Phys. Rev. B **57**, 10248 (1998).
17. S.H. Chun, M.B. Salamon, P.D. Han, Phys. Rev. B **59**, 11155 (1999).
18. W.E. Pickett, D.J. Singh, Phys. Rev. B **55**, R8642 (1997).
19. P. Wagner, I. Gordon, A. Vantomme, D. Dierickx, M.J. van Bael, V.V. Moshchalkov, Y. Bruynseraede, Europhys. Lett. **41**, 49 (1998).
20. M. Ziese, C. Srinitiwarawong, Europhys. Lett. **45**, 256 (1999).
21. P.G. Radaelli, D.E. Cox, M. Marezio, S.-W. Cheong, P.E. Schiffer, A.P. Ramirez, Phys. Rev. Lett. **75**, 4488 (1995).